Solid Earth Discuss., 6, 2215–2259, 2014
www.solid-earth-discuss.net/6/2215/2014/
doi:10.5194/sed-6-2215-2014

Solid Earth
Discussions
Open Access

Low titanium magmatism in northwest region of Paraná continental flood basalts (Brazil): volcanological aspects

F. B. Machado[1], E. R. Viana Rocha-Júnior[2], A. J. Ranalli Nardy[3], and L. Soares Marques[4]

[1]Departamento de Ciências Exatas e da Terra, Universidade Federal de São Paulo, Diadema, SP09920-540, Brazil
[2]Instituto de Física, Universidade Federal da Bahia, Salvador, BA40120-340, Brazil
[3]Departamento de Petrologia e Metalogenia, Instituto de Geociências e Ciências Exatas, Universidade Estadual Paulista, Rio Claro, SP13506-900, Brazil
[4]Instituto de Astronomia, Geofísica e Ciências Atmosféricas, Universidade de São Paulo, São Paulo, SP05508-090, Brazil

Received: 27 June 2014 – Accepted: 14 July 2014 – Published: 4 August 2014

Correspondence to: F. B. Machado (fabio.machado@unifesp.com.br)

Published by Copernicus Publications on behalf of the European Geosciences Union.

Abstract

The early Cretaceous Paraná Continental Flood Basalts (PCFB) is considered as one of the largest volcanic provinces in the world. In Brazil, it completes the last sequence of the sedimentary Paraná Basin (Serra Geral Fm.). The geological unit is contemporary to desert sandstones of Botucatu Fm. and precedes the continental sediments of the Bauru Basin. This Large Igneous Province (LIP) is divided into different types of geochemical magmas which basically are based on TiO_2 content (higher – HTi or lower LTi than 2 wt.% in TiO_2) and incompatible trace elements ratio. Therefore, we studied the magma LTi ($TiO_2 < 2.0$ wt.%), denominated Ribeira which occurs in the northwestern portion of PCFP which is poorly researched mainly in volcanological and geochemical aspects. This basaltic magma, a short expression in PCFB, occurs in the form of multiple pahoehoe flows with thicknesses ranging from 1.5 to 30 m in compound type flows under low surface slope. Peperites zones are common when associated with the first flows, and sand-filled cracks in the lower and upper edges at all pahoehoe levels when in contact with the sediment. Upward these first sequences of interactions with sediment, on the inside direction basin, simple pahoehoe flows occur being associated with Pitanga magma type (HTi, with $TiO_2 > 2.0$ wt.%). Based on rheology data considering anhydrous environment and the composition of plagioclase (An_{42-67}) and clinopyroxene ($Wo_{(30-40)}En_{(34-46)}Fs_{(17-32)}$) showed that the LTi magma is hotter than HTi, with temperatures that range from 1069 °C to 1248 °C while for the second range from 1020 °C to 1201 °C.

1 Introduction

The Serra Geral Fm. ranges the last geological unit of Supersequence Gondwana III in the Paraná Basin, is considered one of the greatest manifestations of intracontinental lavas of the planet and, moreover, the longest spot of continuously exposed rocks of the Brazilian territory. In fact, the fissure magmatism not only shows association with early stages of rupture of southern Pangea and opening of the South Atlantic Ocean (subphase II rift in Almeida et al., 2012), but also substantially altered the modeled in Cenozoic relief in southeastern portion of the South American Platform.

The large volume of basaltic magma is probably greater than 600 000 km^3 in a nearby area of 917 000 km^2 (Frank et al., 2009), reaches 75 % of the Paraná Basin (Fig. 1) covering large areas in south Brazil, Argentina and Uruguay. For Erlank et al. (1984), Duncan et al. (1989), Milner et al. (1995), Marzoli et al. (1999), Marsh et al. (2001), Jerram and Stolhofen (2002), Ernesto et al. (2002), Ewart et al. (2004) and Bryan and Ernst (2008) there are petrological, geochemical and geodynamic evident characteristics in the common genesis involving volcanic activities in South America and those at the Etendeka traps in the west coast of Africa region which consists of the Huab Basin in northwestern Namibia, and further north already in southeastern Angola (Kwanza and Namibe basins).

In the same context, already extrapolating the bounds of the Paraná Basin (Fig. 1) where the formal depositional stratigraphic sequence is named Serra Geral Formation (White, 1908), the magmatism is named Paraná Continental Flood Basalts (PCFB) or Paraná Continental Flood Basalts-Etendeka (e.g. Bryan and Ernst, 2008).

The geochronological research on rocks originated from this volcanic fissure process through Ar^{39}/Ar^{40}, combining with paleomagnetic data, showed that the main ages are between 133 and 132 Ma, with the younger basaltic rocks located in the northern portion of the province, while those oldest in the southern portion according to Müller et al. (1993), Renne et al. (1992, 1996) and Thiede and Vasconcelos (2010) showing therefore that the evolution of volcanic activity in South America occurred from south to north. These same authors have emphasized that probably the largest igneous activity occurred in a close to three million years interval which, in the Ernst (2007) classification, makes the PCFB an example of a Large Igneous Province (LIP).

The great extent of magmatism eventually reflected a petrological heterogeneity in rock types formed showing geochemical and petrographic differences. Concerning the geochemical aspects, systematic studies by Bellieni et al. (1983, 1984ab, 1986ab), Mantovani et al. (1985) and Piccirillo et al. (1987, 1988, 1989) have revealed the existence of two chemically distinct subprovinces based on the concentration of TiO_2, named the high-titanium (HTi, $TiO_2 > 2$ wt.%) and low titanium (LTi, $TiO_2 < 2$ wt.%). The basalts of the first group compared to the second (HTi/LTi) are enriched in Ba (1.88), K_2O (1.38), U (1.20) Sr (2.41) La (2.05), Ce (1.92), Ta (2.43), P_2O_5 (2.54), Hf (1.70) Zr (2.25), TiO_2 (2.46) and depleted in Cs (0.65) and Rb (0.8). In general, those in the HTi group are located in the northern part of the province, above Rio Piquiri Alignment (Fig. 1), the LTi, however, is below the Rio Uruguay Alignment in southern part.

Further, according to the same authors, and using the subsequent names adopted by Peate et al. (1992), HTi subprovince can be divided into three geochemically distinct types magma: HTi(S) or Urubici; HTi(N) or Pitanga, and HTiB or Paranapanema. While LTi subprovince can be divided into three other magma types: LTi(S) or Gramado; LTiB or Esmeralda and LTi(N) or Ribeira. Note that these magmas occur in different geographical regions in the PCFB.

Although this partitioning between subprovinces is an homogeneous majority, according to Piccirillo et al. (1988) and Marques et al. (1989) in the southern portion, LTi, occur HTi rocks (HTi-S or Urubici), with more than 3 % of TiO_2, accounting for only 7 % of all basic igneous activity. Likewise, in the northern part, HTi, rocks of the type LTi (LTi-N or Ribeira) were found, wich were poorly representative in magmatic volume and still understudied.

Therefore, we mainly studied the basaltic flows named of Ribeira magma type, on the petrological and geochemical view including mineral chemistry, of the rocks in the extreme NW of the PCFB in the states of Mato Grosso and Mato Grosso do Sul (Fig. 1) in Brazil. The area is almost devoid of research focusing on the presence of anomalous lava where, to now, only have been reported in samples identified by Piccirillo et al. (1988) and Peate et al. (1992). Furthermore, it becomes important as it represents the most juvenile stage of magmatic province which therefore generates information about the rheology and petrogenesis of basalts associated with the latter stages of the volcanic process. In the same region were also identified samples of basalt HTi, named by the reference cited by Pitanga, where possible genetic relationship with another magma was also verified.

Higher than the deficit of papers on geochemical characterization in this area are studies on the features of interaction between lava and sediment in this region as well as the types of lava occurring. Therefore, we also describe simple and compound pahoehoe flows and different forms of interaction between basic flows and sandstone (sand-filled cracks and peperites) identified only in Ribeira magma type. It is noteworthy that peperite textures as well as various types of interaction, are rare in the northern part of the PCFB being more common in central and southern limits of the basin (Petry et al., 2007; Waichel et al., 2008; Lughetti et al., 2014).

2 Materials and methods

The samples were collected from outcrops of the roads and mining totaling 35 basaltic samples with less than 5 % of alteration minerals. It has become of high importance detailed petrographic analyzes, not only for detection of textures and structures of rocks, but mainly for the selection of samples for geochemical analysis with the least possible alteration minerals which presence would compromise the results.

Geochemical studies were performed in three gradual stages where each one enabled for a filtering of samples for the next stage. The first consisted in obtaining the major, minor and trace elements by X-ray fluorescence, using fused or pressed pellets of powder in borate buffer. All analyzes were performed at the Laboratory of Geochemistry, in Universidade Estadual Paulista, where the analytical error for major elements can reach up to 1.01 % while the traces reach up to 3 %. In the second stage some samples were selected for analysis of rare earth elements (La, Ce, Nb, Sm, Eu, Gd, Dy, Ho, Er, Yb, and Lu) by means of Inductively Coupled Plasma Spectrometry (ICP-MS) using chromatographic separation and ultrasonic nebulizers, where the analytical error is less than 15 %. These analyzes are key for allowing a greater possibility of genetic correlation between the different types of magmas.

Finally, for mineral chemical analysis, approximately 600 points were analyzed (plagioclase – SiO_2, Al_2O_3, TiO_2, Fe_2O_3, MnO, MgO, CaO, SrO, BaO, Na_2O, K_2O; pyroxene – SiO_2, TiO_2, Al_2O_3, Cr_2O_3, FeO, MnO, NiO, MgO, CaO; olivine – SiO_2, TiO_2, Al_2O_3, Cr_2O_3, FeO, MnO, NiO, MgO, CaO, Na_2O; magnetite/ilmenite/titanomagnetite – SiO_2, TiO_2, Al_2O_3, Cr_2O_3, FeO, MnO, MgO, CaO, Nb_2O_5) on representative samples of the types of magmas identified.

3 Geological setting of the study area and sediment-lava interaction

The Botucatu Formation is interpreted like a typical dry aeolian system (e.g. Kocurek and Haveholm, 1993; Sherer et al., 2012), starting in the middle Jurassic (Leonardi and Oliveira, 1990) until the early Cretaceous. Medium to large size tabular cross stratification are common in thin-medium reddish sandstone, with textural bimodality and well selected. Even though it is considered a desert system, it is necessary to clarify the possibility of wet interdune areas, caused by changes in climatic conditions and atmospheric precipitation, which changes the dynamics within the aeolic system, starting with the reduction in the availability of sand likely to be transported. In fact, the highest precipitation causes elevation in the groundwater level and even the formation of interdune deposits between draas.

In this environment, the lavas associated to PCFB, or Serra Geral Fm. in the basin, first filled the areas between dune fields, and then occupied the interdune areas, and finally covered the draas, the largest aeolic accumulations in deserts. The corresponding geological unit in west Africa during the Pangea is Twyfelfontein Fm., in Huab region, formerly known as Etjo Fm.

The contact between both is always concordant and abrupt with absence of paleosols what would indicate any depositional hiatus between the two events. Furthermore, it is evident that the two geological formations are contemporary around the early Cretaceous considering the common intercalations of sandstone in the initial and intermediate sequences, volcanic piles which thickness varies from a few centimeters to almost 10 m in the study area, hence showing short interruptions in the volcanic pulses.

Because of this contemporaneity and youthful appearance of diagenetic stages of the Botucatu Fm sediments in the advent of fissure volcanism, several types of features from the interaction between lava and sedimentary material are apparent. Thus, it was observed the occurrence of peperite zone with approximately 2 m thickness which host sediment is composed by very fine sandstone, silicified and reddish, encompassing irregular clasts of volcanic rock ranging from 4 to 30 cm.

Althogh Jerram and Stollhofen (2002) have discarded the need for wet environment for the formation of peperites (peperite-like), these structures are described as somewhat contentious term currently used to describe a rock formed essentially in situ by disintegration of magma intruding and mingling with unconsolidated or poorly consolidated, typically wet sediments (see reviews by White et al., 2000; Skilling et al., 2002).

The peperite forms in the study are amoeboids and extend up to 80 m. Based on the relative proportions of host sediment and juvenile clast, these peperites have been described as dispersed in internal structure (Skilling et al., 2002). The area occurrence in the region that we studied is always associated to the first spill generating fine sand-filled cracks (up to 1.5 cm) with penetration of up to 30 cm on the overlapping spill (Fig. 2).

It is also worth to emphasize the presence of vesicles oriented according to stratigraphic plan of low angle (5°) or dispersed in the sediment fraction, sediment filling vesicles and fractures in clasts of volcanic rock, and oriented vesicles indicating apparent direction of flow to 25° (pipe-vesicles) (Fig. 2). In fact, these vesicular zones with thickness up to 1 m, are more concentrated in the contact zones with dimensions of up to 2 cm empty or filled by calcite, natrolite or quartz.

Pahoehoe type lava spills are found associated to the earliest pulses from volcanic process with a thickness ranging from 1.5 to 30 m, in compound flows type under surface of low dip, possibly with strings on top, and preserving the Botucatu paleoerg in bypass surface or minor erg warped form.

The individual lobes are small and can reach up to 2.5 m always in the same flow direction as that indicated by the pipe-vesicles. Furthermore, features like characteristics dispersed vesicles and sand-filled cracks in the upper and lower extremities when in contact with the sediment (Figs. 2–4) which we interpret as the P type pahoehoe (Wilmoth and Walker, 1993). Also common is deformation in sedimentary layers because of the weight of overlapping spills by flexural subsidence (Figs. 3 and 4) in a similar situation described by Scherer (2000) in southern PCFB.

In the studied area, the occurrence of sand-filled cracks is always associated to the pahoehoe lava lobes, occurring near the peperite zone (in this case linked to the first flow), or base or tops of upper flows isolated by sediment. Except sandstone in contact with the first flow, others do not have peperite zone, but rocks like breaches composed by fine sediment that in juvenile stage form the sand-filled cracks which can reach up to 10 cm thickness with penetration of up to 3 m in the lower lava flow or that 1 m in upper lava flow.

So, for us the sand-filled cracks are related to fissures that opened during the inflation and subsequent expansion of pahoehoe lava feeder tubes in the extremities in direct contact with the sediment. These filled cracks with fine sandstone, still unconsolidated, can be ascending or descending (Figs. 3 and 4) the latest of which being much more frequent. As opposed to pipe-vesicles, the sand-filled cracks do not necessarily occur in the same direction that the lobes being vertical or inclined. It is noteworthy that sand-filled cracks were also described by Jerram and Stollhofen (2002) in the Awahab Fm. volcanics in Huab Basin.

The base features of pahoehoe in sandstone are rare and have been identified in isolation being more common in slip face regions of the paleodune generating striation marks and chevron marks. Although they have been identified in this study, previous work more focused on sedimentology had previously reported the same occurrence at the northern end of the researched area in Holz et al. (2008).

Finally, the thickness of the flows, as well as all pre-volcanic sedimentary units increases towards the interior of the basin (SW), and near the region of Dourados (Fig. 1) the flows are simple pahoehoe (Fig. 5), massive, and stratigraphically above those compound pahoehoe. The interpretation in relation to thickness and vertical distance of volcanic spills cannot be indicated because of tectonic faults active in the area during the Pleistocene (Fulfaro and Perinoto, 1994), which raised the area and originated Serra do Maraju (Fig. 1) with slopes to the west up to 300 m.

Intrusions are rare, with only two diabase dikes in the southern area close to the latitude of the city of Bonito (Fig. 1), intruded into the base of Botucatu Fm. with direction (NS) parallel to the Arc de Asuncion on W. Also underrepresented, only a diabase sill, approximately 25 km in length was located in the northern area intruded into in the lower portion of the Paraná Supersequence (Fig. 1). This same area, although latest publications by Almeida et al. (2012), with the initial reference to Bellieni et al. (1986) and Peate et al. (1992), indicated the presence of a small swarm of dikes this was not found. This mistake is probably caused by the manner in which this swarm was mapped based almost essentially on interpretation of aeromagnetic data, which may indicate lineaments that do not always reflect structural features related to intrusions of dikes.

Finally, covering the early cretaceous magmatism, in addition to the unconsolidated alluvial and colluvial continental deposits, cenozoic sedimentary rocks occur associated to the Bauru Basin (Fig. 1) in discordant contact with basalts commonly underneath conglomerated supported by basalt clasts, thus indicating erosion process of the upper spills.

4 Petrology aspects

The mineralogy of the investigated rocks is common in the types of flows identified being generally composed by plagioclase, pyroxene (augite and pigeonite) and opaque minerals (magnetite, ilmenite and sulphides). The matrix occurs in microgranular form, being more rarely micrographic (granophyric texture). In subordinate amount it is common the presence of olivine (most often as pseudomorphs) and apatite. There have also been identified alteration minerals like celadonite (quite often), kaolinite, serpentine, biotite, chlorite, calcite and quartz being this last also as primary mineral.

The presence of vesicles is more common in compound pahoehoe flow than in massives, with the presence of structures of segregation in the central portion of the lobes together with microvesicles between plagioclase and pyroxene crystals, defined as diktitaxitic texture, this being indicative of a high volatile content in the magma generator.

As for mineralogical frequency in the basalts of PCFB in NW region of the Paraná Basin, the analysis showed an average of 48.0 % plagioclase, 33.7 % augite, 0.9 % pigeonite, 7.3 % opaque minerals (magnetite, ilmenite), 1.2 % olivine and 7.5 % of microgranular matrix. Among the alteration minerals it is worth to highlight celadonite (1.6 %) and goethite (1.5 %).

The plagioclase crystals have ripiform and prismatic habits, sometimes elongated, with dimensions that range from microcrystals up to 1 mm length. The relation of contact with pyroxene and opaque crystals is made in straight or irregular manner. In many cases, the crystals are shown altered, making it difficult to recognize their twinning, possibly due to the effects of residual fluid circulation (submagmatic stages or hydrothermal alteration in post-crystallization). The alteration of plagioclase crystals occurs at the edges of the mineral and fracture planes generating rings of clay (celadonite and/or kaolinite), or superficial changes in the forms of small blurs on the crystal.

About the pyroxene, there are crystals that range from microlits up to 0.5 mm approximately, being the largest size commonly associated to intrusive bodies. The augite is the most common mineral while pigeonite does not exceed 2 % in volume and may be absent. In addition, many crystals have yellow to reddish blurs on the edges and fracture planes, reaching 10 % of the crystals of goethite-like iron oxide. The meteoric alteration becomes possible because of the composition of up to 6 % FeO in augite and up to 18 % in pigeonite.

Finally, the olivine crystals occur in subhedral to anhedral forms which may show up in a single sample up to 10 % and up to 0.9 mm in length under major axis. In majority it occurs partially or completely substituted by greenish phyllosilicates (possibly celadonite or boulingite), always less than the plagioclase and pyroxene crystals. Petrographic analysis showed that the crystals do not present evidence of reaction edges with other mineral phases, however the fact of crystals having the rounded forms may evidence a reaction of the mineral with the magmatic fluid, which shows indeed the early crystallization compared with other mineral phases.

With this mineral variation influenced by the rheological characteristics of the magma (cooling speed, temperature, viscosity, volatile content, among others), eventually generate a wide variety of textures (Fig. 6). Thus, as intergranular textures, and their subophitic and ophitic variations are associated to rocks with slower cooling because of the prominent formation of mineral phases, this being also the most common in the rocks investigated. Textures of intersertal type (with plagioclase crystals corroded by microgranular matrix), and the graphic texture (characterized by an intergrowth of feldspar and microgranular quartz with vermicular or dendritic forms) also occur whose occurrence in itself is already indicative of magmatic differentiation processes, with separation of residual liquid rich in volatile forming anomalous mineral phases even in a basic lava.

5 Geochemistry aspects

The samples were classified according to the criteria proposed by the Subcommittee on Systematics of Igneous Rocks (Le Bas et al., 1986) in TAS diagram (SiO_2 vs. Alkali), Fig. 7, being all of them located in basalt field, with silica concentrations ranging from 50.04 wt.% to 53.34 wt.%. Also, according to the classification of Zanettin (1984) can be considered in majority tholeiitic and subalcaline second Bargar and Irvine (1971). Exception must be made to only two samples displaced toward the basaltic andesite field.

Still, through the diagram A ($Na_2O + K_2O$)–F ($Fe_2O_{3(t)}$)–M (MgO) it is also possible to observe the sub-alkaline and tholeiitic nature of basalts investigated (Fig. 8). All samples are above the Irvine and Baragar (1971) line in tholeiitic field. This trend can also be confirmed by the modal mineralogy, with the presence of two pyroxenes (augite and pigeonite) and the presence of quartz and hypersthene, as shown by the results of the CIPW norm in samples considered as representative in Table 1.

The chemical data for major and minor elements of the samples on anhydrous basis were studied in diagrams having MgO as the only index of magmatic fractionation (Fig. 9), where it is clearly observed that with the decrease of MgO there is an increase in the concentrations of all elements except Al_2O_3 and CaO. Also, all basalt samples have MgO ranging from 3.31 wt.% to 6.51 wt.% while the SiO_2 ranges from 50.04 wt.% to 53.34 wt.%, the trends of magmatic evolution appear to be well defined for Al_2O_3 (12.45 wt.% to 14.10 wt.%), CaO (7.71 wt.% to 10.45 wt.%), K_2O (0.72 wt.% to 1.87 wt.%), Na_2O (2.12 wt.% to 2.73 wt.%) and P_2O_5 (0.18 wt.% to 0.68 wt.%).

It is noteworthy that the concentrations of Al_2O_3 are variable (SD of up to 0.3 on average concentration of 12.81 wt.%) for a similar degree of magmatic fractionation with MgO presenting SD of 0.15 and average concentration of 4.10 wt.%, what should probably reflect different degrees of fusion as interpreted by Hirose and Kushiro (1993) for the geochemical behavior of this element in magmatic systems through analytical and experimental methods.

The TiO_2 separates at least two well defined groups, a less enriched in this element with 1.68 wt.% to 2.05 wt.% (3.31 wt.% $<$ MgO $<$ 3.72 wt.%) and the other with 3.58 wt.% to 4.18 wt.% (5.25 wt.% $<$ MgO $<$ 6.51 wt.%). Some samples show intermediate values in this element with TiO_2 between 2.20 wt.% and 3.23 wt.%. Even so, the data for this element are already indicative of the presence of two groups: HTi and LTi (Table 1).

Finally, the $Fe_2O_{3(t)}$ has values ranging from 13.07 wt.% to 17.00 wt.%, a group more depleted in this element stands out with concentration less than 14.17 wt.%, more enriched in MgO than the others and equivalent depleted group in TiO_2 (LTi). Sharing again the interpretation of Hirose and Kushiro (1993), the element in question is not affected by the degree of partial melting, is significantly sensitive to the pressures under which the fusion takes place, and its concentration is higher in the magma generator in conditions of higher pressure. On the other hand, differences in the values may suggest that fusion occurred in regions of the mantle already depleted in this element due to melting processes in the past.

When the trace elements, diagrams elaborated again with MgO as an index of magmatic evolution (Fig. 10) show that with the increase in concentration of this element there is a decrease in the concentration of La, Ba, Ce, Rb. Zr, Y, Nb and Sr. All the samples investigated have La ranging from 8 $\mu g\,g^{-1}$ to 51 $\mu g\,g^{-1}$, Ba from 234 $\mu g\,g^{-1}$ to 645 $\mu g\,g^{-1}$, Ce from 25 $\mu g\,g^{-1}$ to 134 $\mu g\,g^{-1}$, Rb from 13 $\mu g\,g^{-1}$ to 37 $\mu g\,g^{-1}$, Y from 25 $\mu g\,g^{-1}$ to 48 $\mu g\,g^{-1}$ and Nb from 8 $\mu g\,g^{-1}$ to 30 $\mu g\,g^{-1}$. It is noteworthy that only one sample has anomalous concentration of Rb (42 $\mu g\,g^{-1}$) which may represent possible crustal contamination processes, since this alkali metal is essentially volatile and is typical of sialic crust.

It also makes evident the individuation of LTi and HTi groups to Zr and Sr, where the first group corresponds to a variation of 111 $\mu g\,g^{-1}$ to 138 $\mu g\,g^{-1}$, and 246 $\mu g\,g^{-1}$ to 286 $\mu g\,g^{-1}$ respectively, while the second group has a range of 228 $\mu g\,g^{-1}$ to 275 $\mu g\,g^{-1}$, and 246 $\mu g\,g^{-1}$ to 286 $\mu g\,g^{-1}$ respectively.

With this, it is possible that the detailing of these groups which fundamentally lead to TiO_2 concentration for the different magmas in nomenclature adopted by Peate et al. (1992). The HTi group is represented by Pitanga magma type, more enriched in TiO_2 (2.67–4.18 wt.%), P_2O_5 (0.30–0.68 wt.%), Sr (396–437 $\mu g\,g^{-1}$), Ba (344–645 $\mu g\,g^{-1}$), Zr (169–175 $\mu g\,g^{-1}$), and depleted in SiO_2 (50.04–51.52 wt.%) and $Fe_2O_{3(t)}$ (13.07–15.98 wt.%) compared to the LTi samples which are represented by the Ribeira magma. Likewise, the ratios of the trace elements are also higher Ti/Y (544–677), Zr/Y (5–7), Ti/Zr (554–677), Sr/Y (9–16) and Ba/Y (13–18).

For the Ribeira magma type on its turn, presents the following changes in concentration: SiO_2 (50.67–51.87 wt.%), TiO_2 (1.68–2.63 wt.%), $Fe_2O_{3(t)}$ (13.10–17.00 wt.%), P_2O_5 (0.18–0.33 wt.%), Sr (246–286 $\mu g\,g^{-1}$), Ba (344–645 $\mu g\,g^{-1}$), Zr

(169–175 $\mu g\, g^{-1}$), and ratios between traces: Ti/Y (320–414), Zr/Y (4–5), Ti/Zr (320–414), Sr/Y (6–10) and Ba/Y (7–10). The variation in the different concentrations of magma, by its importance and individuality in the basin is shown in Table 2 and Fig. 11.

It is noteworthy that, as previously described, the Ribeira samples are also more primitive in MgO, with concentrations ranging from 4.22 wt.% to 6.51 wt.%, in comparison to those of Pitanga type, with 3.44 wt.% to 5.85 wt.%. This magma LTi is associated with flows described as pahoehoe in the base of the volcanic pile, while those in HTi are located at the interior of the basin.

With little occurrence among identified geochemical groups, were also identified some samples with intermediate concentrations between the two groups described, these being closest to Paranapanema classification (Fig. 11). However, the concentrations of TiO_2, Sr, $Fe_2O_{3(t)}$ or the ratios between traces, are not conclusive and neither permit the individualization of this group, but may be linked to different degrees of magmatic evolution between the other two magma types or just one of them.

When fifteen samples selected by geographical location and variation in MgO (some represented in Table 1) are recorded in multi elementary diagram (Fig. 12), in general, the basalts are characterized by exhibiting moderate fractionation of light REE, with ratios $(La/Yb)_n$ ranging from 4.2 to 7.7, $(La/Sm)_n$ from 2.2 to 2.5, and $(Sm/Yb)_n$ from 1.8 to 3.1, in addition to light anomalies of Eu/Eu* (0.94 to 1.08).

In general, it is also made evident that the Ribeira samples have lower enrichment in light REE (mean ratio $(La/Yb)_n = 5.6 \pm 1.7$) than those from Pitanga (ratio average $(La/Yb)_n = 6.1 \pm 1.5$). Furthermore, Pitanga samples show to be more enriched in rare intermediary earth in relation to heavy ($(Sm/Yb)\ n = 2.6 \pm 0.6$) than those from Ribeira ($(Sm/Yb)\ n = \pm\ 2.3 \pm 0.6$). All samples from Ribeira have a positive Eu anomaly, while the ones from HTi are slightly positive or negative.

When considering the patterns of abundance of incompatible elements of the basalts studied, there is a clear similarity between the magmas as shown in Fig. 13. In the same figure, the magma Pitanga has higher enrichment in all elements when compared to Ribeira, with the following average ratios: Rb/Rb*(49), Ba/Ba*(67), Th/Th*(41), U/U*(37), K/K*(48), Ta/Ta*(42), Nb/Nb*(29), La/La*(49), Ce/Ce*(42), Sr/Sr*(22), Nd/Nd*(29), P/P*(23), Hf/Hf*(27), Zr/Zr*(28), Sm/Sm*(20), Eu/Eu*(17), Ti/Ti*(26), Tb/Tb* (12), Y/Y* (8) and Yb/Yb*(7).

The Ribeira, however, presents average ratios: Rb/Rb*(29), Ba/Ba*(36), Th/Th* (24), U/U*(21), K/K*(26), Ta/Ta*(23), Nb/Nb*(13), La/La*(24), Ce/Ce*(20), Sr/Sr*(11), Nd/Nd*(14), P/P*(9), Hf/Hf*(15), Zr/Zr*(16), Sm/Sm*(10), Eu/Eu*(9), Ti/Ti*(13), Tb/Tb* (7), Y/Y* (6) and Yb/Yb*(6).

6 Mineral chemistry aspects

For the quantification of the chemical composition of the main mineral phases fifteen samples Pitanga (HT) and ten samples Ribeira (LTI) magma type were selected, the choice was also based on the abundance of each type of basalt where two of those LTi are intrusive and all others extrusive.

The study of evolution and compositional variations of plagioclase was based on the relationship between albite (Ab) – anorthite (An) – orthoclase (Or) and the structural formula calculation was used the formula proposed by Deer et al. (1997), employing eight oxygen atoms.

However, the results show that it is not possible to distinguish between two types of magmas using signatures of this mineral. The composition generally ranges from labradorite to andesine (An42-67 – 14A), reaching An1 in samples enriched with granophyric matrix with presence of crystals of potassium feldspar of later crystallization (Fig. 6d). Microphenocrystal core for both types of magma presents more calcium composition, located in the field in labradorite with An ranging from 53 % to 67 %. The crystals of late development, or edges and intermediate zones are more sodic with An ranging from 42 % to 53 % in the field of andesite as shown by diagram in Fig. 14b.

For the classification of clinopyroxenes (augite and pigeonite) we used the method proposed by Morimoto et al. (1988), where they are divided into four groups: Ca-Mg-Fe (Quad) Ca-Na, Na and others. For the initial classification, we used the parameters

$Q(Ca + Mg + Fe^{+2})$ vs. $J(2Na)$ based on the total number of cations in the octahedral positions M1 and M2. As shown by the diagram in Fig. 15a all samples are located in the Quad field, which allowed us to determine the ternary diagram Wo-En-Fs (Fig. 15b). The structural formula used is that published in the cited references, being based on six oxygen atoms and four cations.

Thus, when the clinopyroxenes of the Quad field are plotted on the diagram Wo-En-Fs (Fig. 15b), we observe that they present, mostly, calcium pyroxene compositions of augite type, and in least abundant form the pigeonite type.

The augite crystals ($Wo_{(30–40)}En_{(34–46)}Fs_{(17–32)}$) are present not only at the edges of pigeonite, but mainly as integral crystals, with no compositional difference between the center and edge. The crystals of Ribeira sample tend to be less calcic ($Wo_{30–40}$) than those of Pitanga magma type ($Wo_{37–40}$).

Pigeonite crystals investigated have composition $Wo_{(10–12)}En_{(51–55)}Fs_{(35–39)}$, determined in isolated crystals and sometimes partially or completely enveloped by augite, showing serrated contact. The Ribeira samples shown in Fig. 15, have up to 2 % pigeonite and show an enrichment in Mg ($En_{\sim 52}$) of this mineral phase. Difference occurs with pigeonite of Pitanga samples, with less than 0.5 % of this mineral and less enriched in Mg (En_{35}) also represented in the diagrams.

Ultimately, it is also evident in the diagrams of Fig. 15 that the clinopyroxenes associated to Ribeira basalt have tendency to a composition closer to enstatite, therefore more magnesian than those in Pitanga magma type.

Still using the pyroxenes, in the Ca-Mg-Fe* diagram the crystals of augite, for both types of magmas, analyzed at the center and edge of microphenocrystals, define well defined trend parallel to the Skaergaard line (Fig. 16). The edges and intermediate points of crystals of augite and pigeonite show enrichment in Fe* and depletion of Ca when compared to the centers of these minerals.

For the olivine crystals the majority is located in the intermediate field between the end members forsterite-fayalite, specifically in field hortonolite Fo ~ 31–50, except for one Pitanga sample with Fo ~ 60. The gradual enrichment in SiO_2 and the concomitant decrease of Fo show a greater degree of magmatic evolution in the Pitanga samples relative to Ribeira magma type.

The opaque crystals showed the coexistence of magnetite and ilmenite with no correlation between the habit and the chemical composition in which, using the geothermometer from Stormer (1983) and based on the two magmas identified, those crystals relating to Ribeira have a crystallization temperature ranging from 922 °C to 970 °C, much higher than those of Pitanga magma with 823 °C to 853 °C.

It is also observed that, utilizing the method of Andersen and Lindsley (1985), the Ribeira magma type has a relatively greater fugacity ($-11{,}00 > fO_2 > -11{,}72$) than Pitanga magma type samples ($-12{,}98 > fO_2 > -13{,}57$).

Considering now the pyroxene to calculate the temperature in accordance to Lindsley (1983), the coexistence of pigeonite and augite in the rocks can be used to estimate the temperature of crystallization of these minerals (Fig. 17). Coprecipitation of augite and pigeonite occurred between 900 °C to 1000 °C approximately. The same diagram also suggests that the Ribeira magma type samples have crystallization temperature of clinopyroxenes even reaching 1150 °C, greater than those of Pitanga magma type, lower than 1090 °C.

Yet for pyroxene, now utilizing the Kretz geothermometer (1982), the Pitanga magma type has an augite crystallization at a temperature ranging from 1135 °C to 1201 °C, also lower than the Ribeira magma type between 1201 °C to 1248 °C.

However, assuming an anhydrous scenario, and utilizing the constitution of plagioclase just from extrusive samples to Mathez geothermometer (1973), it was possible to verify an interval of 1020 °C to 1055 °C for Pitanga magma and 1069 °C to 1095 °C for Ribeira magma. That is, the tendency for the higher temperature LTi magma persists in this method of calculation, different from the others, which use the zero value water pressure.

Thus, using the latter geothermometer and also of the Kretz (1982) for pyroxene, it also becomes evident that the range of the crystallization plagioclase temperature is much lower than that for pyroxene, there is no concomitant crystallization of these two minerals in either of the types of magmas (Table 3).

7 Conclusions

In this study, we conclude that in the NW portion of PCPB the first flows are associated to Ribera magma type (LTi), pahoehoe type, with thicknesses ranging from 1.5 to 30 m, in compound flows type under low surface slope. In the first spill there may occur peperite zone, which extends up to 80 m in a single outcrop, generating volcanic blocks with amoeboid forms hosted in sedimentary rock. In the contact it was also possible to identify pipe-vesicles indicating an apparent direction of lava into 25°.

Although the occurrence of peperites, by definition, is related to wet areas, the Botucatu Fm. was a big hot desert system, high-pressure, with estimated area of 1.3 million km^2 which would be, especially in its boundaries, more exposed to climatic conditions active during the Jurassic to early Cretaceous. Thus, the sedimentary environment, even local, would be conditioned to basically three factors: atmospheric (especially during the volcanism that may have altered the ambient pressure); geographical position (the limits of the desert would be in areas of climatic transition); and nearby mountains (which may have created conditions for the existence of fluvial channels that could eventually have attained proximal desert areas). Thus, if we admit these parameters, we would explain the occurrence of the described peperites with the possibility of a connected wet environment.

Furthermore, it was also described the occurrence of sand-filled cracks associated to compound pahoehoe flow, formed by very fine sandstone, with thickness up to 10 cm and penetration of 3 m in the lower spill or 1 m in the upper spill related to the sand layer generated. For us the occurrence is related to fissures that opened during the inflation and subsequent expansion of pahoehoe lava feeder tubes in the extremities in direct contact with the sediment. These fissures filled with fine sandstone, still unconsolidated, not only demonstrate that the lithostatic weight of the upper spill directly influence the upward injection of the material but also show that the Botucatu Fm. was still far from complete diagenetic process during volcanic event.

In fact, this interpretation corroborates one of the hypotheses described by Jerram and Stolfens (2002), and is based on the generation model of this type of lava described by Self (1997). The occurrence of sand filled cracks has no direct relationship with the peperites zones occurrence, but yes to the type of lava associated.

If on the one hand, the sills and the first flows at NW PCFB are associated with the Ribeira type, occurring at the boundary between the volcanic unit and Botucatu Fm, on the other hand younger lavas are associated to Pitanga magma type (HTi), always simple massive pahoehoe, being interpreted as subsequent because of the fact that it is located in most regions within the basin. Interpretations about thicknesses and vertical distances from the volcanic piles could not be precisely indicated because of active tectonic faults acting in the area during the Pleistocene. In the affected area, in outcrops, when compared to the whole PCFB, the Ribeira magma type represents approximately 0.3 % of the volcanic event.

The studied rocks are basalts with silica concentrations ranging from 50.04 wt.% to 53.34 wt.%, tholeiitic and subalkaline. Ribeira samples have a lower enrichment in light REE (average ratio $(\mathrm{La/Yb})n = 5.6 \pm 1.7$) than those Pitanga (average ratio $(\mathrm{La/Yb})n = 6.1 \pm 1.5$). Furthermore, Pitanga samples were more enriched in intermediate REE compared to the heavy ($(\mathrm{Sm/Yb})n = 2.6 \pm 0.6$) than those Ribeira ($(\mathrm{Sm/Yb})n = 2.3 \pm 0.6$). When considering the patterns of abundance of incompatible elements of the basalts studied, also normalized by primordial mantle, there is an evident similarity between the magmas where magma Pitanga has greater enrichment in all elements when compared to the Ribeira. This similarity in the geochemical behavior of traces suggests cogenicity in the mantle source and the action of dissimilar magmatic processes.

The mineral chemism data showed that the composition for plagioclase varies from labradorite to andesine (An42-67) and that it is not possible to distinguish the two types of magmas identified. For the pyroxene, pigeonite crystals investigated have composition $Wo_{(10–12)}En_{(51–55)}Fs_{(35–39)}$, whereas crystals of augite ($Wo_{(30–40)}En_{(34–46)}Fs_{(17–32)}$) are present not only at the edges of pigeonite, but mainly as whole crystals. The Ribeira sample crystals tend to be less calcic ($Wo_{30–40}$) than those of Pitanga type ($Wo_{37–40}$). The olivine, generally, is situated in the intermediate field between the end members forsterite-fayalite, more precisely in hortonolite field with $Fo_{\sim 31–50}$.

As for calculating the crystallization temperatures, in anhydrous environment, the Ribeira magma is always the one with the highest temperature than the Pitanga. For the LTi, considering the plagioclase and the clinopyroxene and assuming that there was no concomitant crystallization of these two minerals, it was calculated from 1069 °C to 1248 °C while for the HTi it was 1020 °C to 1201 °C.

Acknowledgements. This study was supported by FAPESP (04/10081-9 e 05/51818-7) and CNPq. We thank Breno Leitão Waichel, Mario Assine and Alexandre Perinotto by the stimulating discussions about Serra Geral Fm. and sediment interaction. This is a GEO-SEDex – USP contribution (No. 05).

References

Almeida, F. F. M., Carneiro, C. S. R., and Bartorelli, A.: Magmatismo pós-paleozoico no Brasil, in: Geologia do Brasil, Beca edn., edited by: Hasui, Y., Carneiro, C. D. R., Almeida F. F. M., and Bartorelli, A., 430–452, 2012.

Bellieni, G., Brotzu, P., Comin-Chiaramonti, P., Ernesto, M., Melfi, A. J., Pacca, I. G., Piccirilo, E. M., and Stolva, D.: Petrological and paleomagnetic data on the plateau basalts to rhyolite sequencies of the southern Paraná Basin (Brazil), An. Acad. Bras. Ciênc., 55, 355–383, 1983.

Bellieni, G., Comin-Chiaramonti, P., Marques, L. S., Melfi, A. J., Piccirilo, E. M., Nardy, A. J. R., and Roisenberg, A.: High- and low-Ti flood basalts from the Paraná Plateou (Brazil): petrology end geochemical aspects bearing on their mantle origin, Neues Jb. Miner. Abh., 150, 272–306, 1984a.

Bellieni, G., Comin-Chiaramonti, P., Marques, L. S., Melfi, A. J., and Stolfa, D.: Low-pressure evolution of basalt sills from bore-holes in the Paraná Basin, Brazil, TMPM, 33, 25–47, 1984b.

Bellieni, G., Comin-Chiaramonti, P., Marques, L. S., Martinez, L. A., Melfi, A. J., Nardy, A. J. R., Piccirilo, E. M., and Stolva, D.: Continental flood basalts from central-western regionas of the Paraná Plateau (Paraguay and Argentina): petrology and petrogenetic aspects, Neues Jb. Miner. Abh., 154, 11–139, 1986a.

Bellieni, G., Comin-Chiaramonti, P., Marques, L. S., Melfi, A. J., Nardy, A. J. R., Papatrechas, C., Piccirillo, E. M., and Roisenberg, A.: Petrogenetic aspects of acid and basaltic lavas from the Paraná Plateau (Brazil): geological, mineralogical and petrochemical relationships, J. Petrol., 27, 915–944, 1986b.

Bryan, S. E. and Ernst, R. E.: Revised definition of Large Igneous Provinces (LIPs), Earth-Sci. Rev., 86, 175–202, 2008.

CPRM: Companhia de Pesquisa e Recursos Minerais, Mapa Geológico de Mato Grosso do Sul, escala 1:1 000 000, Brasília, 2006.

Deer, W. A., Howie, R. A., and Zussman, J.: Rock Forming Minerals, An Introduction to the Rockforming Minerals, 2nd edn., Longman Group Limited, London, 1997.

Duncan, A. R., Neuwton, S. R., Van Den Berg, C., and Reid, D. L.: Geochemistry and petrology of dolerite sills in the Huab River valley, Damaraland, north western Namibia, Communications of the Geological Survey of Namibia, 5, 5–18, 1984.

Erlank, A. J., Marsh, J. S., Duncan, A. R., Miller, R. M. C. G., Hawkesworth, C. J., Betton, P. J., and Rex, D. C.: Geochemistry and petrogenesis of the Etendeka volcanic rocks from SWA/Namibia, in: Petrogenesis of the Volcanic Rocks of the Karoo Province, vol. 13, edited by: Erlank, A. J., Special Publication of the Geological Society of South Africa, 195–245, 1984.

Ernesto, M., Marques, L. S., Piccirillo, E. M., Molina, N., Ussami, P., Comin-Chiaramonti, G. P., and Bellieni, P.: Paraná magmatic province – Tristan da Cunha plume system: fixed vs. mobile plume, petrogenic considerations and alternative heat sources, J. Volcanol. Geoth. Res., 118, 15–36, 2002.

Ernst, R. E.: Mafic–ultramafic Large Igneous Provinces (LIPs): importance of the pre-Mesozoic record, Episodes, 30, 107–113, 2007.

Ewart, A., Marsh, J. S., Milner, S. C., Duncan, A. R., Kamber, B. S., and Armstrong, R. A.: Petrology and geochemistry of early cretaceous bimodal continental fllod volcanism of the NW Etendeka, Namibia. Part 1: Introduction, mafic lavas and re-evaluation of mantle source components, J. Petrol., 45, 59–105, 2004.

Frank, H. T., Gomes, M. E. B., and Formoso, M. L. L.: Review of the extent and the volume of the Serra Geral Formation, Paraná Basin, South America, Pesquisas em Geociências, 36, 49–57, 2009.

Fulfaro, V. J. and Perinotto, J. A. J.: A tectônica fanerozóica no Mato Grosso do Sul: o graben de Corguinho e a Formação Ponta Porã, in: Anais do IV Simpósio de Geologia do Centro-Oeste, 61–63, 1994.

Hirose, K. and Kushiro I.: Partial melting of dry peridotites at high pressures: determination of compositions of melts segregated from peridotite using aggregates of diamond, Earth Planet. Sc. Lett., 114, 477–489, 1993.

Holz, M., Soares, A. P., and Soares, P. C.: Preservation of aeolian dunes by pahoehoe lava: an example from the Botucatu Formation (Early Cretaceous) in Mato Grosso do Sul state (Brazil), western margin of the Parana' Basin in South America, J. S. Am. Earth Sci., 25, 398–404, 2008.

Irvine, T. N. and Baraguar, W. R. A.: A guide to the chemical classification of the common volcanic rocks, Can. J. Earth Sci., 8, 523–548, 1971.

Jerram, D. A. and Stollhofen, H.: Lava-sediment interaction in desert settings; are all peperite-like textures the result of magma-water interaction?, J. Volcanol. Geoth. Res., 114, 231–249, 2002.

Kocurek, G. and Haveholm, K. G.: Eolian sequence stratigraphy – a conceptual framework, in: Siliciclastic Sequence Stratigraphy – Recente Developments and Applications, vol. 58, edited by: Weimer, P. and Posamentier, H., American Association of Petroleum Geologists, AAPG Memoir, Tulsa, 393–409, 1993.

Kretz, R.: Transfer exchange equilibrium in a portion of the pyroxene quadrilateral as deduced from natural and experimental data, Geochim. Cosmochim. Ac., 46, 411–421, 1982.

Le Bas, M. J., Le Maitre, R. W., Streckeisen, A., and Zannetin, B.: A chemical classification of volcanic rocks based on total alkali-silica diagram, J. Petrol., 27, 745–750, 1986.

Leonardi, G. E. and Oliveira, F. H.: A revision of the Triassic and Jurassic tetrapod footprints of Argentina and a new approach on the age and meaning of Botucatu Formation footprints (Brazil), Revista Brasileira de Geociências, 20, 216–229, 1990.

Lindsley, D. H.: Pyroxene thermometry, Am. Mineral., 68, 477–493, 1983.

Luchetti, A. C. F., Nardy, A. J. R., Machado, F. B., Madeira, J. E. O., and Arnosio, J. M.: New insights on the occurrence of peperites and sedimentary deposits within the silicic volcanic sequences of the Paraná Magmatic Province, Brazil, Solid Earth, 5, 121–130, 2014.

Mantovani, M. S. M., Marques, L. S., Souza, M. A., Atalla, L., Civeta, L., and Inonocenti, F.: Trace element and strontium isotope constrains of the origin and evolution of Paraná coantinental flood basalts of Santa Catarina State (Southern Brazil), J. Petrol., 26, 187–209, 1985.

Marques, L. S., Piccirilo, E. M., Melfi, A. J., Comin-Chiaramonti, P., and Bellieni, G.: Distribuição de terras raras e outros elementos traços em basaltos da Bacia do Paraná, Geochimica Brasiliensis, 3, 33–50, 1989.

Marsh, J. S., Ewart, A., Milner, S. C., Duncan, A. R., Miller, R. and Mc, G.: The Etendeka Igneous Province: magma types and their stratigraphic distribution with implications for the evolution of the Paraná–Etendeka flood basalt province, B. Volcanol., 62, 464–486, 2001.

Marzoli, A., Melluso, L., Morra, V., Renne, P. R., Sgrosso, I., D'Antonio, M., Duarte Morais, L., Morais, E. A. A., and Ricci, G.: Geochronology and petrology of Cretaceous basaltic magmatism in the Kwanza basin (western Angola), and relationships with the Paraná–Etendeka continental flood basalt province, J. Geodyn., 28, 341–356, 1999.

Mathez, E. A.: Refinement of the Kudo Weill plagioclase discrimination thermometer and its application to basaltic rocks, Contrib. Mineral. Petr., 41, 61–72, 1973.

McBirney, A. R. and Noyes, R. M.: Crystallization and layering of the Skaergaard intrusion, J. Petrol., 20, 487–554, 1975.

McDonough, W. F. and Sun, S. S.: The composition of the Earth, Chem. Geol., 120, 223–254, 1995.

Milner, S. C., Duncan, A. R., Whittingham, A. M., and Ewart, A.: Trans-atlantic correlation of eruptive sequences and individual silicic volcanic units within the Paraná–Etendeka igneus province, J. Volcanol. Geoth. Res., 69, 137–157, 1995.

Morimoto, N., Fabries, J., Fenguson, A. K., Ginzburg, I. V., Ross, M., Seifert, F. A., Zussyman, J., Aoki, K., and Gottardi, G.: Nomenclature of pyroxenes, Mineral. Mag. J. M. Soc., 52, 535–550, 1988.

Müller, R. D., Royer, J., and Lawver, L. A.: Revised plate motions relative to the hotspots from combined Atlantic and Indian Ocean hotspots tracks, Geology, 191, 27–53, 1993.

Peate, D. W., Hawkeswort, C. J., and Mantovani, M. S. M.: Chemical stratigraphy of the Paraná lavas (South America): classification of magma types and their spatial distribution, B. Volcanol., 55, 119–139, 1992.

Petry, K., Jerram, D. A., Almeida, D. del P. M., and Zerfazz, H.: Volcanic-sedimentary features in the Serra Geral Fm., Paraná Basin, southern Brazil: examples of dynamic lava-sediment interactions in an arid setting, J. Volcanol. Geoth. Res., 159, 313–325, 2007.

Piccirillo, E. M., Raposo, M. I. B., Melfi, A. J., Comin-Chiaramonti, P., Bellieni, G., Cordani, U. G., and Kawashita, K.: Bimodal fissural volcanic suítes from the Paraná Basin (Brazil): K-Ar age, Sr-isotopes and geochemistry, Geochimica Brasiliensis, 1, 53–69, 1987.

Piccirillo, E. M., Comin-Chiaramonti, P., Melfi, A. J., Stolfa, D., Bellieni, G., Marques, L. S., Giaretta, A., Nardy, A. J. R., Pinese, J. P. P., Raposo, M. I. B., and Roisenberg, A.: Petrichemistry of continental flood basalt-rhyolite suites and related intrusives from the Paraná Basin (Brazil), in: The Mesozoic Flood Volcanism of the Paraná Basin: Petrogenetic and Geophysical Aspects, edited by: Piccirillo, E. M. and Melfi, A. J., Universidade de São Paulo, 107–156, 1988.

Piccirillo, E. M., Civetta, L., Petrini, R., Longinelli, A., Bellieni, G., Comin-Chiaramonti, P., Marques, L. S., and Melfi, A. J.: Regional variations within the Paraná flood basalts (southern Brazil): evidence for subcontinental mantle heterogeneity and crustal contamination, Chem. Geol., 75, 103–122, 1989.

Renne, P. R., Ernesto, M., Pacca, I. G., Coe, R. S., Glen, J. M., Prévot, M., and Perrin, M.: The age of Paraná flood volcanism, rifting of Gondwanaland, and the Jurassic–Cretaceous boundary, Science, 258, 975–979, 1992.

Renne, P. R., Deckart, K., Ernesto, M., Féraud, G., and Piccirillo, E. M.: Age of the Ponta Grossa dike swarm (Brazil), and implications to Paraná flood volcanism, Earth Planet. Sc. Lett., 144, 199–211, 1996.

Scherer, C. M. S.: Eolian dunes of the Botucatu Formation (Cretaceous) in Southernmost Brazil: morphology and origin, Sediment. Geol., 137, 63–84, 2000.

Skilling, I. P., White, J. D. L., and McPhie, J.: Peperite: a review of magma-sediment mingling, J. Volcanol. Geoth. Res., 114, 1–17, 2002.

Stormer, J. C. J.: The effects of recalculation on estimates of temperature and oxygen fugacity from analyses of multicomponent irontitanium oxides, Am. Mineral., 68, 586–594, 1983.

Thiede, D. S. and Vasconcelos, P. M.: Paraná flood basalts: rapid extrusion hypothesis confirmed by new ^{40}Ar/^{39}Ar results, Geology, 38, 747–750, 2010.

Waichel, B. L., Scherer, C. M. S., and Frank, H. T.: Basaltic lava flows covering active aeolian dunes in the Paraná Basin in southern Brazil: features and emplacement aspects, J. Volcanol. Geoth. Res., 171, 59–72, 2008.

White, J. D. L., McPhie, J., and Skilling, I. P.: Peperite: a useful genetic term, B. Volcanol., 62, 65–66, 2000.

Wilmoth, R. H. and Walker, G. P. L.: P-type and S-type pahoehoe: a study of vesicle distribution patterns in Hawaiin lava flows, J. Volcanol. Geoth. Res., 55, 129–142, 1993.

Zanettin, B.: Proposed new chemical classification of volcanic rocks, Episodes, 7, 19–20, 1984.

Table 1. Analysis of representative samples of the basalts from NW region of the PCFB. For the CIPW norm, it was considered the $FeO/(FeO + Fe_2O_3) = 0.85$ ratio.

	Low-Ti							High-Ti
Magma type	Ribeira	Ribeira	Ribeira	Ribeira	Ribeira	Ribeira	Ribeira	Pitanga
Form	Lava	Lava	Lava	Lava	Lava	Lava	Lava	Lava
Sample	KS 739	KS 741	KS 743	KS 745	KS 779	KS 830	KS 841	KS 742
SiO_2	51.23	51.87	50.77	50.32	50.32	51.14	50.06	50.12
TiO_2	1.84	2.40	2.20	2.98	2.70	2.63	3.96	3.82
Al_2O_3	13.87	13.07	13.36	13.81	13.58	12.45	12.81	12.91
Fe_2O_3	13.10	15.21	15.02	13.57	15.31	17.00	16.07	15.57
MnO	0.21	0.23	0.22	0.19	0.22	0.24	0.23	0.24
MgO	6.05	4.24	5.54	5.75	5.03	4.22	3.89	4.45
CaO	10.45	9.07	9.34	9.65	9.05	8.44	7.76	8.59
Na_2O	2.23	2.57	2.31	2.38	2.31	2.38	2.49	2.57
K_2O	0.82	1.05	0.99	1.04	1.11	1.18	2.14	1.33
P_2O_5	0.21	0.28	0.25	0.33	0.37	0.31	0.59	0.40
Total	100.00	100.00	100.00	100.00	100.00	100.00	100.00	100.00
quartz %	10.95	9.69	12.67	10.59	9.35	9.42	9.88	11.22
zircon	0.02	0.03	0.04	0.03	0.03	0.02	0.03	0.05
orthoclase	5.05	4.83	6.18	5.86	4.98	4.40	5.66	9.75
albite	18.42	18.86	21.76	19.54	18.98	18.55	18.32	22.11
anorthite	24.38	25.44	21.06	23.20	23.92	24.80	24.01	18.23
diopside	15.12	15.28	11.56	11.58	15.48	15.36	15.04	4.22
hypersthene	7.21	7.99	5.20	8.43	8.60	8.81	8.14	8.11
olivine	0.12	0.12	0.30	0.17	0.15	0.12	0.09	0.05
chromite	0.03	0.02	0.02	0.03	0.02	0.04	0.02	0.01
magnetite	14.17	13.10	15.21	15.02	13.91	14.06	14.16	15.42
ilmenite	0.49	0.45	0.49	0.46	0.47	0.45	0.49	0.47
titanite	3.78	3.92	5.26	4.80	3.87	3.74	3.87	9.22
apatite	0.50	0.50	0.67	0.59	0.50	0.47	0.49	1.39
Total	100.24	100.23	100.42	100.30	100.26	100.24	100.20	100.25
Nb	8	13	14	12	13	9	9	22
Zr	114	138	176	158	134	123	127	246
Y	26.0	31.0	45.0	35.0	25.0	28.5	29.1	43.0
Sr	246	277	285	280	262	281	276	398
Rb	19	13	22	25	25	16	22	27
Zn	89	81	94	98	88	87	86	117
Cu	115	108	344	206	109	167	143	209
Ni	55	57	38	46	53	68	54	26
Cr	135	94	87	117	113	177.4	113	47
Ce	35	27	42	46	33	37	32	86
Ba	256	274	341	336	302	261	279	578
La	19	15	19	27	25	21	19	33

Table 2. Ribeira and Pitanga geochemical signatures of basaltic magmas in NW PCFB region.

Magma type	Pitanga – High-Ti		Ribeira – Low-Ti	
	minimum	maximum	minimum	maximum
SiO_2	50.04	51.52	50.67	51.87
TiO_2	2.67	4.18	1.68	2.63
$Fe_2O_{3(t)}$	13.07	15.98	13.10	17.00
MgO	3.44	5.85	4.22	6.51
P_2O_5	0.30	0.68	0.18	0.33
Zr	169	275	111	210
Sr	396	438	246	286
Ba	344	645	234	424
Ti/Y	554	677	320	414
Zr/Y	5	7	4	5
Ti/Zr	554	677	320	414
Sr/Y	9	16	6	10
Ba/Y	13	18	7	10

Table 3. Different temperatures, and differences between minimum and maximum (Δ), calculated by geothermometers for the basaltic magmas Ribeira (LTi) and Pitanga (HTi) in NW PCFB region.

			Opac Minerals		Pyroxenes				Plagioclase	
			Stormer (1983)	Δ	Lindsley (1983)	Δ	Kretz (1982)	Δ	Mathez (1973)	Δ
LTi	Ribeira	max	970 °C	48	1150 °C	100	1248 °C	47	1095 °C	26
		min	922 °C		1050 °C		1201 °C		1069 °C	
HTi	Pitanga	max	853 °C	30	1090 °C	190	1201 °C	66	1055 °C	35
		min	823 °C		900 °C		1135 °C		1020 °C	

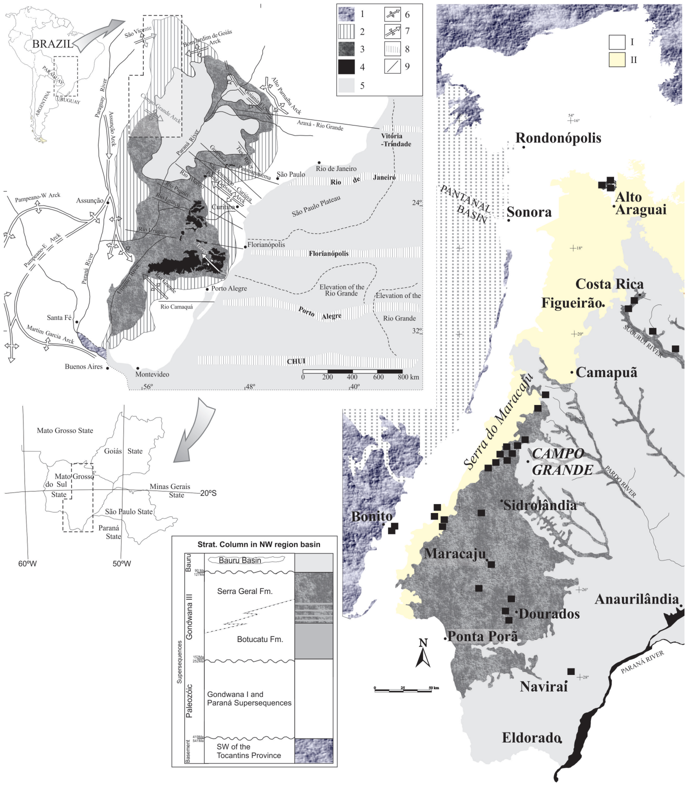

Figure 1. Simplified Geological map (CPRM, 2006) of the studied area with the location of samples collect. In systematization: geological map of the Paraná Basin, Brazilian states involved in research and Stratigraphic Column of the area. 1 – Tocantins Province area (basement), 2 – pre-volcanic sedimentary rocks; 3 – basalts (Serra Geral Formation) 4 – acid members (Serra Geral Formation); 5 – post-volcanic sedimentary rocks (Bauru Basin), 6 – anticlinal structure; 7 – synclinal structure; 8 – oceanic Lineaments; 9 – continental lineaments, I – Paleozoic sequences of the Paraná Basin; II – Botucatu Formation.

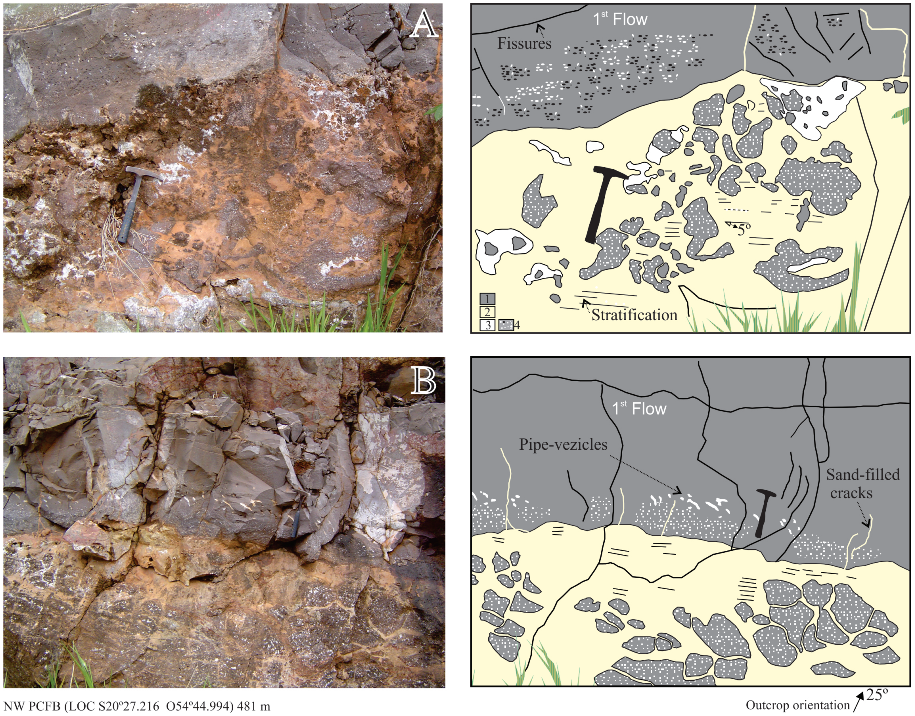

Figure 2. Details of outcrops near peperite zone with flow breccia horizons with clasts of volcanic rock in the aeolic sandstone. **(A)** Peperite texture in very fine sandstone with stratification plane parallel with juvenile volcanic clasts with amoeboid form and sand-filled crack in the base of lava. **(B)** Pipe vesicles next to peperite zone com sand-filled crack. (1) Basalt. (2) Botucatu Fm. (3) Calcite precipitation. (4) Clasts with vesicle bands.

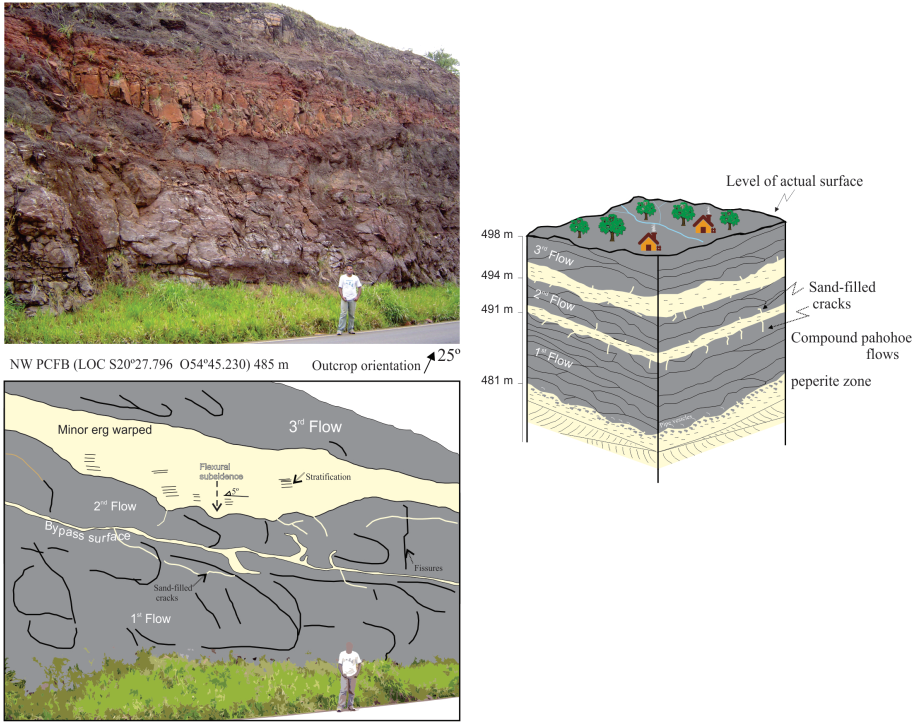

Figure 3. Intercalated P-type pahoehoe lava flows, with compound lobes, separated by layers of sandstone (Botucatu Fm.) with features like bay-pass and minor erg warped.

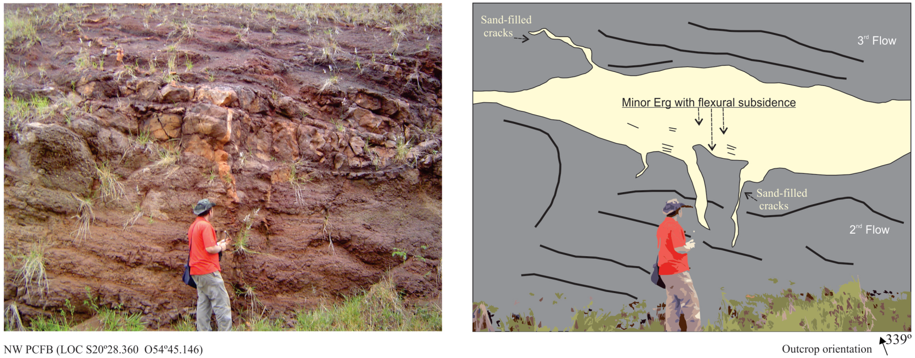

Figure 4. Outcrop with ascending and descending sand-filled cracks in two pahoehoe lava flows separated by Botucatu Fm. sediment.

NW PCFB (LOC S22º06.660 O54º47.700) 399 m

Figure 5. Simple pahoehoe flows in mining in the region researched, near the city of Dourados (Fig. 1) area. In the top image, location of the point in relation to geographic north (quickboard image from Google Earth).

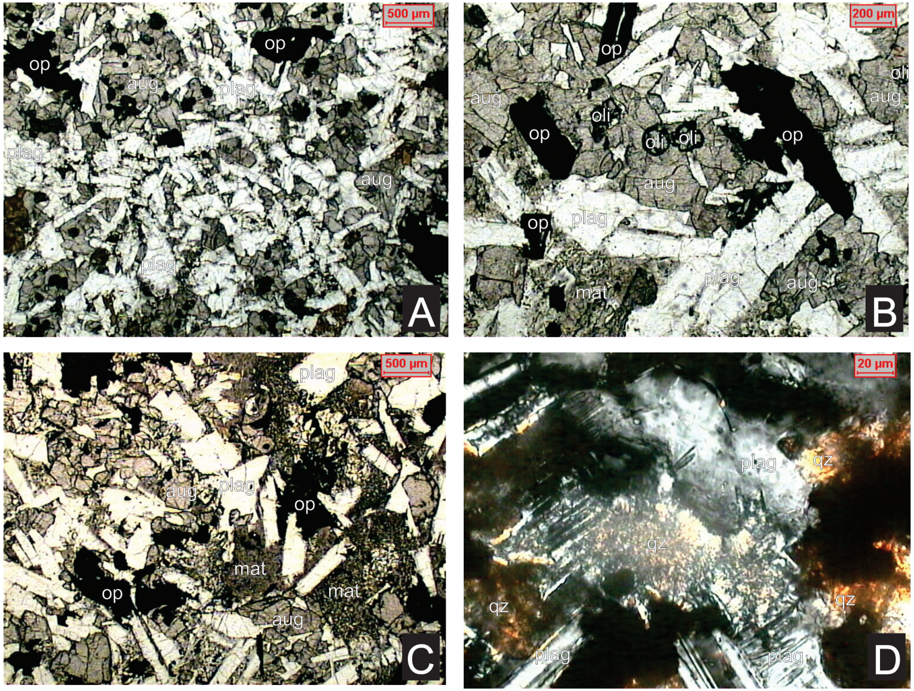

Figure 6. Different textures identified in basaltic samples collected in the area studied. **(A)** Intergranular with plagioclase subhedral crystals with interstitial augite crystals (parallel nicols). **(B)** Subophitic with plagioclase crystals partially included in crystals of augite (parallel nicols). **(C)** Intersertal with plagioclase crystals corroded by the matrix (parallel nicols). **(D)** Graphic, with fuzzy aspect micrographic matrix containing quartz (crossed nicols). Legend: plag – plagioclase; aug – augite; op – opaque minerals (magnetite/ilmenite); mat – matrix; oli – olivine.

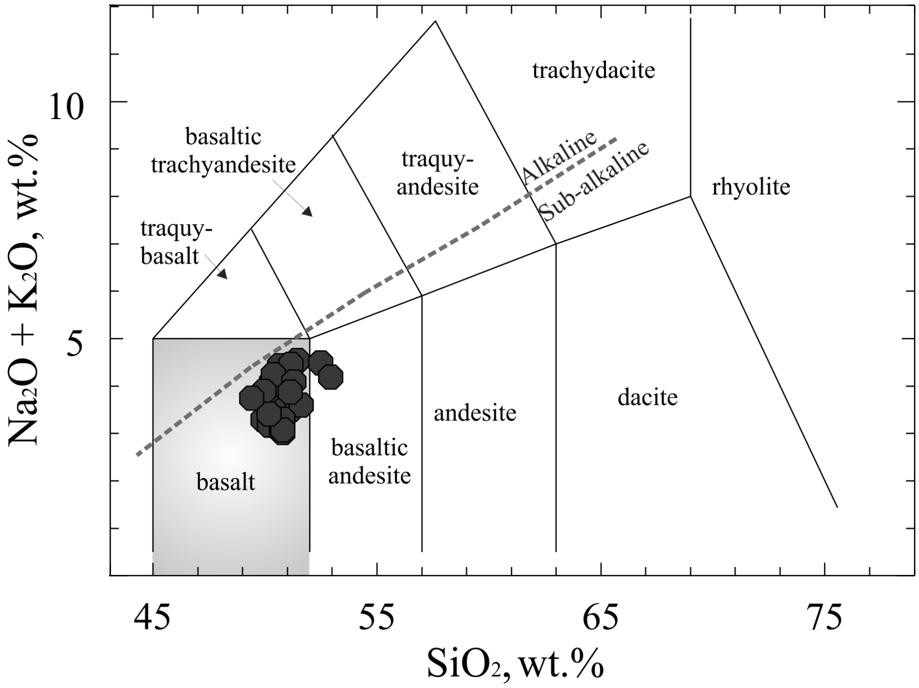

Figure 7. TAS diagram classification of rocks (Le Bas et al., 1986) for basalts investigated. The dotted line separates the fields of the alkaline and sub-alkaline rocks (Baragar and Irvine, 1971).

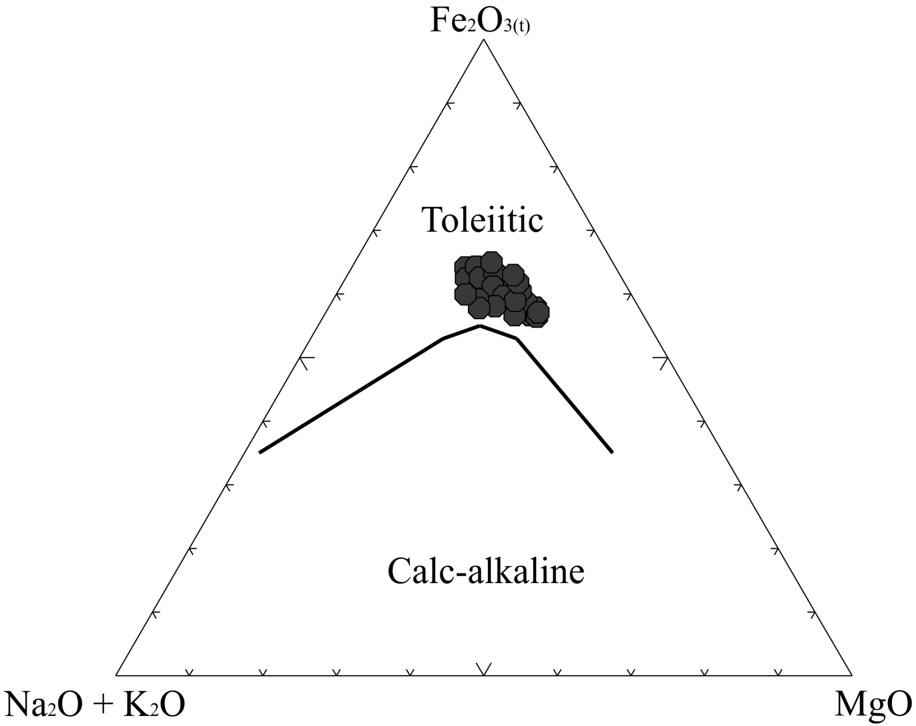

Figure 8. AFM diagram (A – $Na_2O + K_2O$ – F – $Fe_2O_{3(t)}$ – M – MgO), showing tholeiitic character of the studied basalts (Irvine and Baragar, 1971).

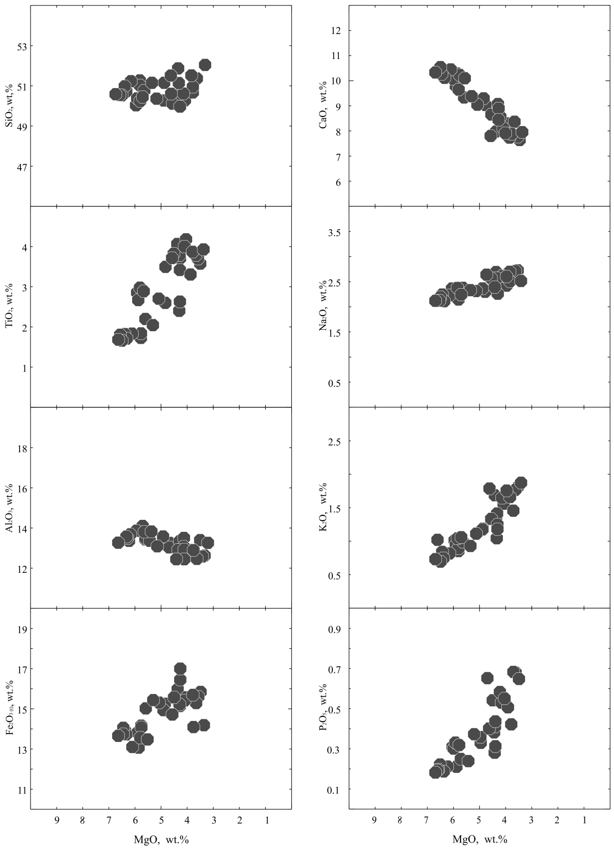

Figure 9. Variation diagrams of major and minor elements (wt.%) vs. MgO (wt.%) in investigated basalts.

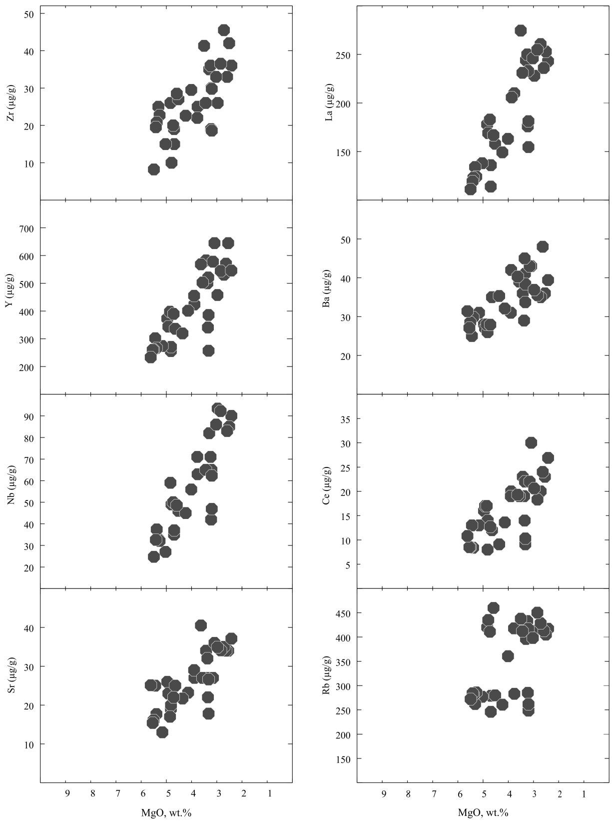

Figure 10. Variation diagrams of trace elements (µg g^{-1}) vs. MgO (wt.%) in basalts investigated.

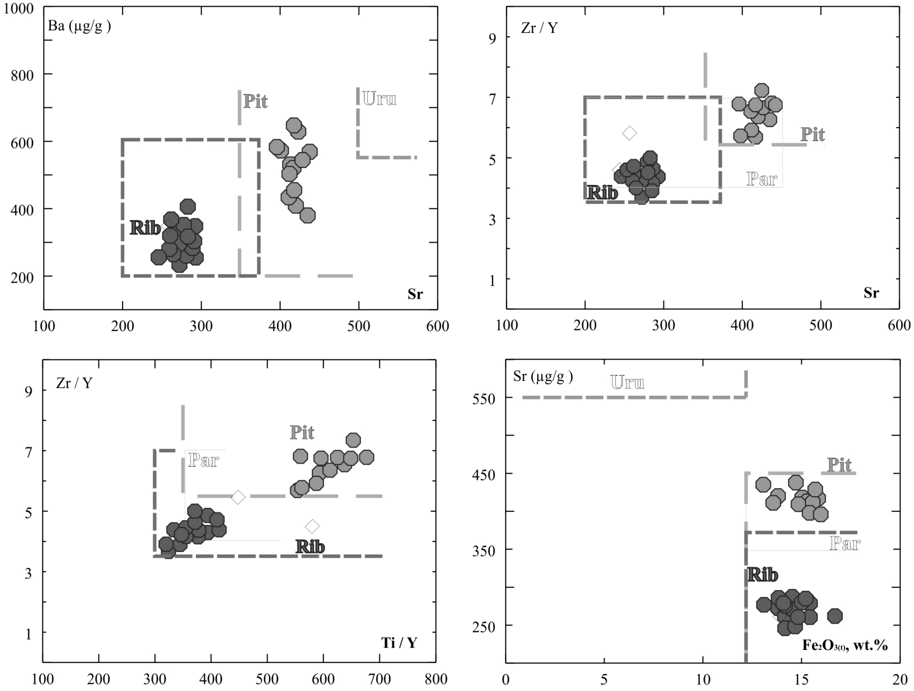

Figure 11. Behavior of the samples investigated in discriminatory diagrams of the types of magmas of basaltic flows from PCFB by Peate (1997). Pit – pitanga; par – paranapanema; rib – ribeira; uru – urubici; rhombus samples – undefined.

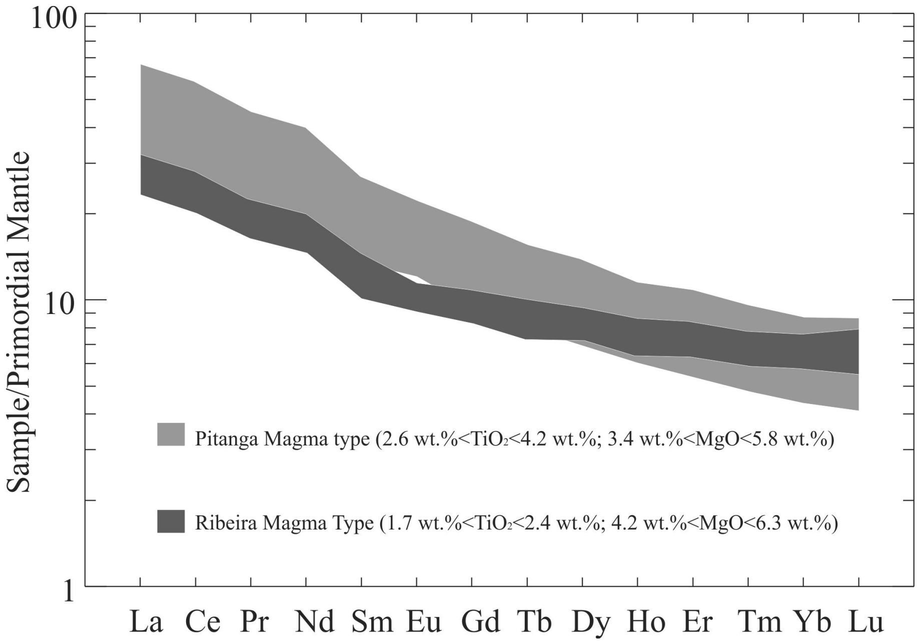

Figure 12. Distribution diagram of REE elements showing the range of variation of concentrations of Pitanga and Ribeira magmas. Values normalized in relation to primordial mantle of Sun and McDonough (1995).

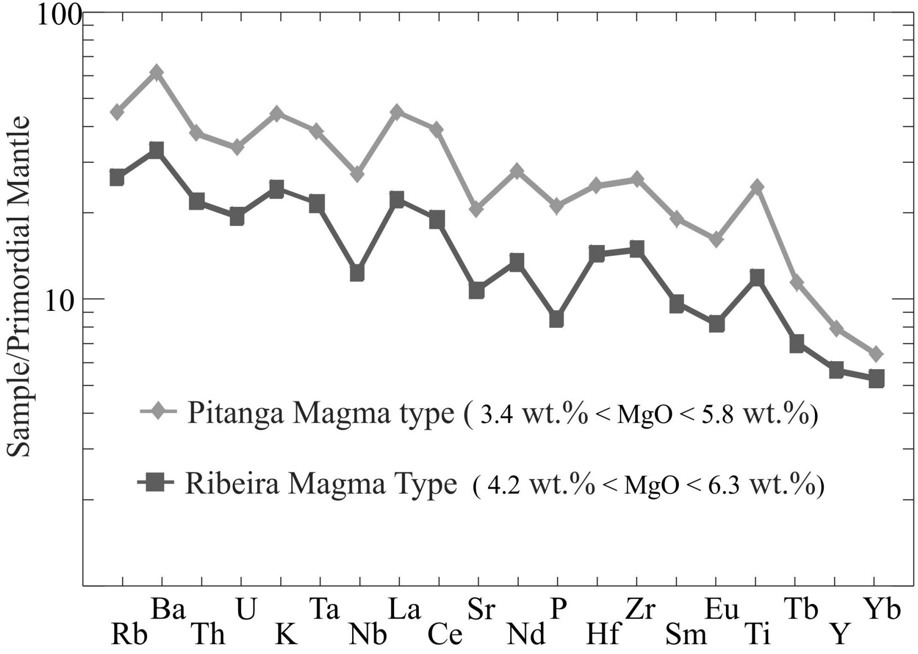

Figure 13. Incompatible element diagram normalized in relation to primordial mantle (McDonough and Sun, 1995). The ratios plotted in the diagram represent the average calculated for different samples of Ribeira and Pitanga basalt investigated. Note general similarities between Pitanga and Ribeira magma types.

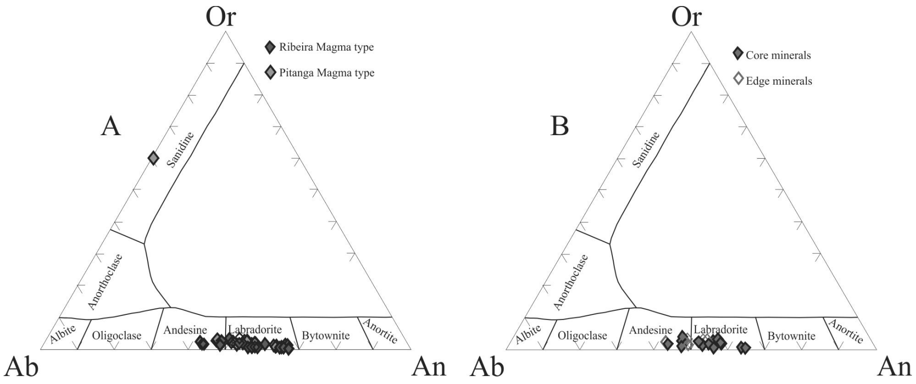

Figure 14. Diagram Ab-An-Or with the classification of feldspars in basalts investigated for both types of magma identified **(A)** and analysis in microphenocrystal core and edge for both magmas **(B)**, the geochemical variation observed was from labradorite to andesine mineral.

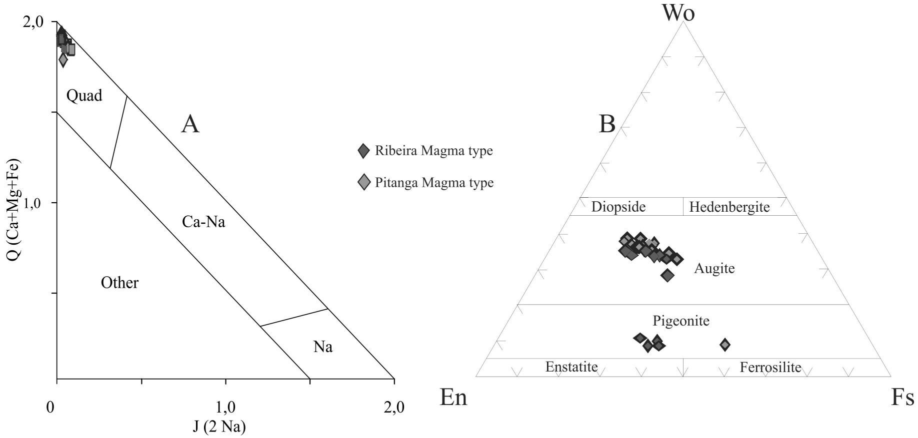

Figure 15. Morimoto et al. (1988) diagrams : Q–J **(A)** where all the pyroxenes analyzed are located in the Quad field, and Wo-En-Fs **(B)** with the classification of clinopyroxenes from different samples analyzed.

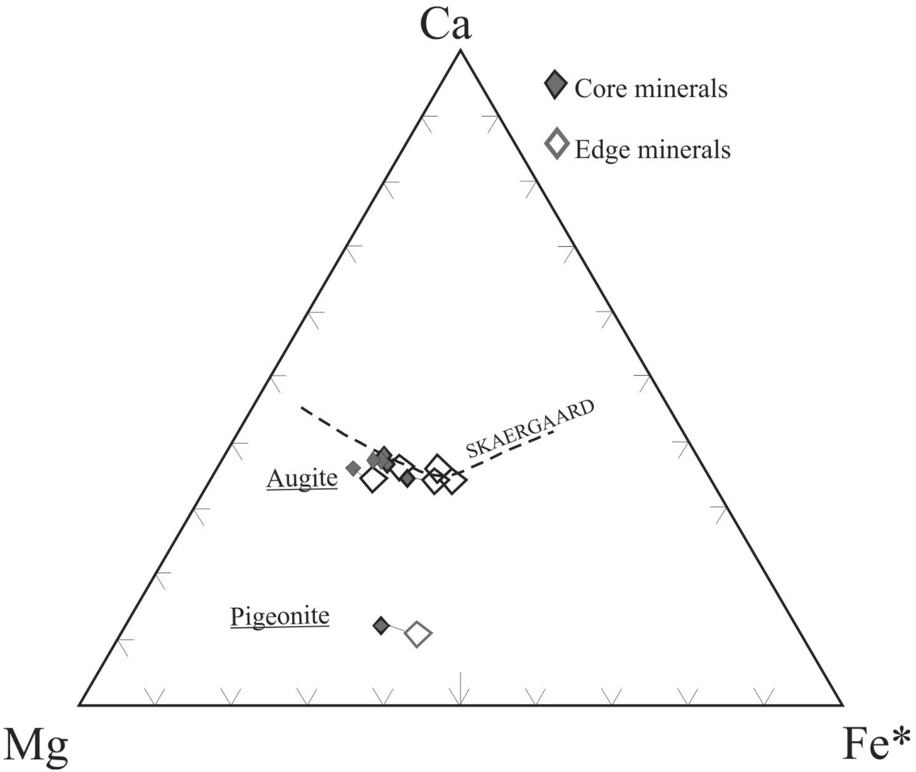

Figure 16. Diagram Ca-Mg-Fe* ($Fe^* = Fe^{2+} + Fe^{3+} + Mn$) with pyroxene crystals analyzed in the center and edge, forming trend (augite) parallel to Skaergaard line by McBirney and Noyes (1975).

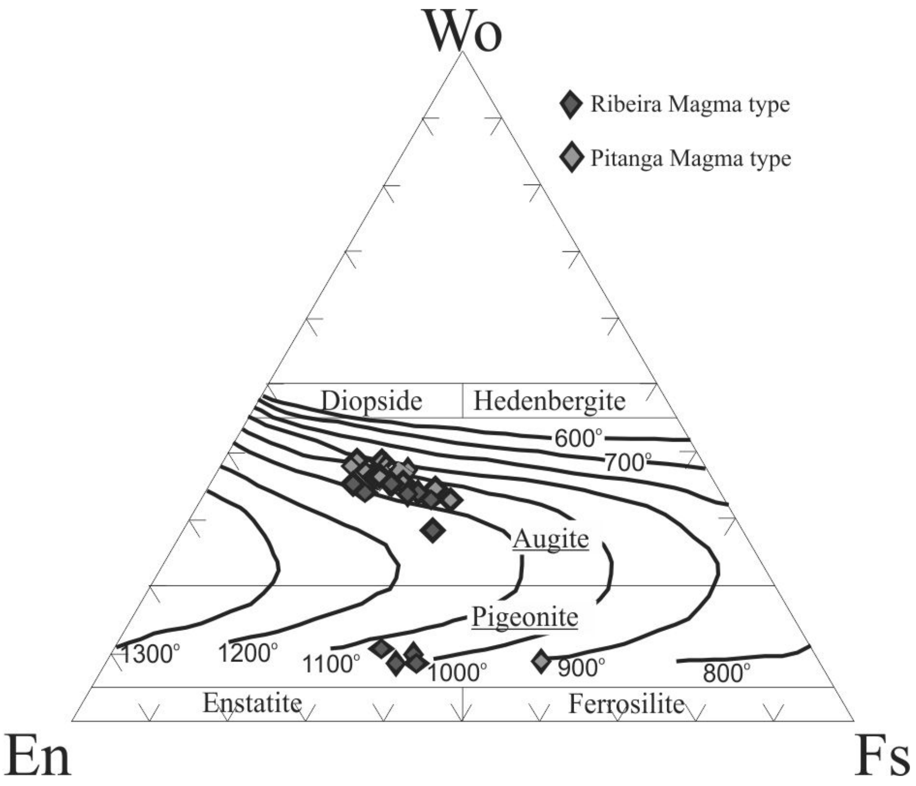

Figure 17. Wo-En-Fs diagram with all analyzes of pyroxene plotted and isotherms adapted from Linsley (1983).